

# Melt Homogenization Improvement During The Bridgman Crystal Growth Optimizing The Rotation Profile

V. Tabouret<sup>1</sup>, J. Petit<sup>1</sup>, B. Viana<sup>2</sup>

<sup>1</sup> Onera, the French Aerospace Lab, Chatillon, FRANCE

<sup>2</sup> Institut de Recherche de Chimie Paris/CNRS, Paris, FRANCE

**Abstract:** A fluid dynamics analysis and solution homogenization in a Bridgman-Stockbarger furnace was studied. We aimed to optimize the use of the furnace to elaborate single crystals for non-linear laser applications in the mid infrared. This paper describes the study of the influence of different rotation profiles on the homogenization for improved crystal growth.

**Keywords:** Bridgman furnace, crystal growth, solution homogenization.

## 1. Introduction

One goal of our work is to find and process crystals for non-linear laser applications in the mid infrared<sup>1, 2, 3</sup> (ie. 3 $\mu$ m-13 $\mu$ m). We are interested by two major applications: *i*) optical counter measure for aircraft security<sup>4</sup>, *ii*) remote gas sensing. The studied crystals have to be transparent in the infrared, should present a high non-linear optical coefficient and good thermal properties to increase the laser power<sup>6, 7</sup>. We have already recently elaborated AgGaS<sub>2</sub>, ZnGeP<sub>2</sub> and AgGaGeS<sub>4</sub> single crystals<sup>8, 9, 10</sup>. The process used can be described in two steps: *i*) the synthesis of the compounds from the reaction of the elements (Zn, Ge...), *ii*) the single crystal growth. In order to be used in optical devices, the single crystal quality has to be high. We have to use high temperature ( $\approx 1100^{\circ}\text{C}$ ) to melt our compounds but some volatile elements appear and cause a modification of the species' concentration into the melt<sup>11</sup>. So the compound has to be confined in ampoule for instance. This permits also to protect the material from oxidation.

To grow crystals in an ampoule, we used the Bridgman-Stockbarger method<sup>11, 12</sup>, where a melted compound is slowly cooled with a vertical movement through a gradient of temperature. In a Bridgman-Stockbarger furnace, the high temperature zone is on the top, which does not allow good thermal convection in the melt. Moreover, inhomogeneity can appear in the melt, either by the departure of volatile compounds or directly by the

crystallization when the chemical compositions in the melt and the crystal are different<sup>10</sup>. In order to help the homogenization of the fluid, a rotation of the ampoule, which contains the melt, is used. Usually, the rotation has a constant speed (named as CR for Constant Rotation) but, in order to improve the homogenization, a system which can modulate the profile of the rotation's speed is proposed (named as VR, for Variable Rotation).

So, the goal of this study is to optimize the homogenization in the Bridgman-Stockbarger furnace. First, we will describe our system and our model. Then, we will present the calculation results about the difference of homogenization behavior between CR profiles and VR profiles. Next, we will present the optimization of the VR profiles. Finally, we will show the influence of the viscosity on the model because viscosity is an unknown experimental parameter that should be determined by other experimental measurements.

## 2. System's description

The core of the Bridgman furnace is a cylinder where a crucible moves vertically in a temperature gradient. A scheme of the furnace with a filled ampoule is shown in the Figure 1. The profile of temperature was experimentally measured in the furnace by a translating thermocouple. The ampoule is either in CR or in VR mode: it is fixed over a ceramic arm which transmits rotation and translation movements.

Three coupled physics are used in the model: (i) fluid mechanics, (ii) heat transfer and (iii) transport of diluted species. The software used to model the system is COMSOL Multiphysics<sup>TM</sup> which provides a modeling platform for coupling various physics. The variation of viscosity and density (which are not constant because of the thermal inhomogeneity of the system) paired with a high Reynold number (5000) required a 3D numerical solution to the Navier-Stokes equations. Our compound has also to be melted over  $1000^{\circ}\text{C}$ , so the thermal radiation has

to be taken into account (the ampoule is considered to be opaque to this radiation). The module Transport of Diluted Species was used to consider the homogenization of the melt.

To model the homogenization in the fluid, an arbitrary diluted species (with no chemical reaction) is used. Once the system reached a steady-state, we fixed two volumes with two different concentrations. This moment is considered as the initial time. The aim is to observe the evolution of the concentration map. Several simplifications in the model can be done: as the movement in the temperature gradient is slow (near  $1\text{mm}\cdot\text{h}^{-1}$ ) and the studied time is short (150s), the crystallization of the melt (phase change) is not considered in this work in order to decrease the calculation time. The vertical movement is considered as negligible in the model too.

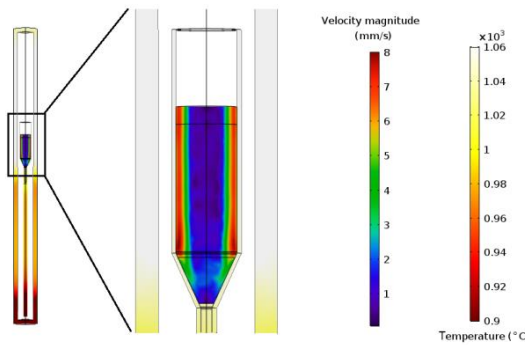


**Figure 1:** Scheme of the filled ampoule in the furnace (showing the temperature profile along the walls, and the rotation speed in the liquid, with an ampoule rotation of 12rpm)

### 3. Governing equations

Because of the high value of the Reynold number (close to 5000) and the viscosity (described in table 2), the flow has to be considered as turbulent. The fluid model used is the “low Reynold k-epsilon model”, which solves the equations from the Reynold Average Navier Stockes model (RANS – model). This fluid model is frequently used in the industry to model incompressible fluid systems.

As the ampoule is placed in a temperature gradient, the density and viscosity are not homogenous in the ampoule. The equations used to describe this thermal evolution are the following (the equation of the viscosity derives from the Arrhenius equation<sup>13</sup>):

$$\mu = \mu_0 e^{1000 \cdot (1/T - 1/T_0)} \quad (1)$$

$$\rho = \frac{\rho_0}{1 + \alpha(T - T_0)} \quad (2)$$

Where  $\mu$  corresponds to the viscosity at the temperature  $T$ ,  $\mu_0$  to the viscosity at the temperature  $T_0$ .  $\rho$  stands for the density at the temperature  $T$ .  $\alpha$  stands for the coefficient of thermal expansion.

With the equations of heat transfer and fluid mechanics, we can study the movement of the fluid in the ampoule. The transport model used to describe the situation is a combination of the Fick law and convection, with no chemical reaction (Equation 3).  $C$  stands for the concentration of the diluted species,  $D$  stands for the diffusion coefficient and  $\mathbf{u}$  stands for the velocity field in the melt.

$$\frac{\partial c}{\partial t} + \nabla \cdot (-Dc) + \mathbf{u} \cdot \nabla c = 0 \quad (3)$$

## 4. Numerical model in Comsol Multiphysics

### 4.1 Mesh and geometry

A coarse mesh (size of elements between 3 and 15cm) is used for the furnace’s walls, because we have considered quite smooth profile temperature. A “boundary limit layer” mesh is used in the melt with respect to the ampoule speed variation. A fine mesh (size of elements between 0.8 and 4cm) is used in the fluid. The meshed geometry in the ampoule is shown in Figure 2:

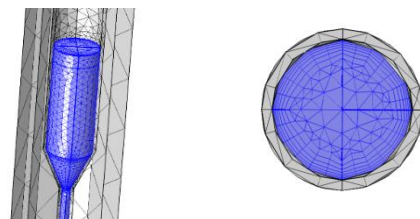


**Figure 2:** Meshing in the model, the blue part corresponds to the fluid

### 4.2 Sizes of the system

The geometric parameters of the system are presented in Table1.

Name	Symbols	Values [mm]
Inner furnace radius	$R_{col}$	792

Height of the furnace	$H_{col}$	21.7
Inner large cylinder radius of the ampoule	$R_{max}$	15.7
Inner small cylinder radius of the ampoule	$R_{min}$	4.45
Thickness of the ampoule	$e_p$	2
Height of the small cylinder of the ampoule	$h_q$	44.8
Height of the large cylinder of the ampoule	$h_r$	100
Height of the ampoule	$h_t$	169.3
Height of the column	$h_{cb}$	380

**Table 1:** Geometric parameters

### 4.3 Melt parameters

The studied compounds ( $ZnGeP_2$ ,  $AgGaGeS_4$ ) have some unknown parameters especially at high temperature, so we have to take some values reported in the literature from better known compounds. As Germanium is present in our compounds and have a fusion temperature close to the chosen compounds, we decided to take the viscosity value of pure Germanium at its fusion temperature as viscosity reference<sup>13</sup>. The density value comes from the density of  $ZnGeP_2$  at ambient temperature. The values are given in Table2.

Name	Symbols	Values
Viscosity reference <sup>14</sup>	$\mu_o$	0.73[mPa.s]
Density reference	$\rho_o$	4500[kg.m <sup>-3</sup> ]
Expansion's coefficient of the fluid	$a_{ex}$	$1.10^{-4}[K^{-1}]$

**Table 2:** Melt parameters

### 4.4 Thermal parameters

The value of the thermal conductivity of the fluid comes from melted Germanium<sup>15</sup>. We used the values of alumina for the cylinder under the ampoule and of silica for the ampoule. Because of the high temperature in the model which is near 1100°C, we have to take into account the furnace's radiation. The values are presented in Table 3. The experimental temperature profile is shown in the Figure 3 and was imposed along the furnace walls in the model.

Name	Symbols	Values
Thermal conductivity of the fluid <sup>15</sup>	$k_l$	59.9[W.m <sup>-1</sup> .K <sup>-1</sup> ]
Heat capacity of the fluid <sup>15</sup>	$C_{p_l}$	447.6[J.kg <sup>-1</sup> .K <sup>-1</sup> ]
Heat capacity of the ampoule	$C_{p_s}$	700[J.kg <sup>-1</sup> .K <sup>-1</sup> ]
Density of the ampoule	$\rho_s$	2329[kg.m <sup>-3</sup> ]
Surface emissivity of the furnace and the ampoule	$\epsilon_m$	0.45

**Table 3:** Thermal parameters

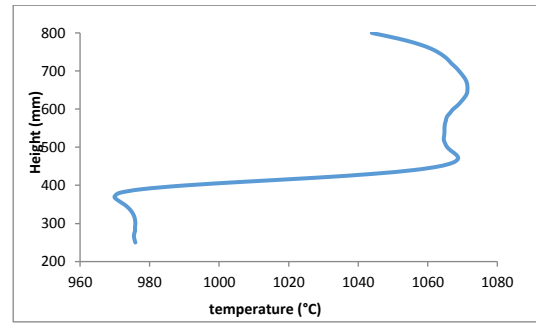


**Figure 3:** Temperature at the walls of the furnace (with a cylindrical symmetry)

### 4.5 Two steps of calculation

The simulation has two steps of calculation: At first, the transport of diluted species is not considered. This allows the system to be in thermal and fluid equilibrium state. In the second part, the transport of diluted species with the inhomogeneity of concentration is considered, to study the homogenization in the system.

## 5. Results and Discussion

The first step was to compare the two types of rotation profiles, CR and VR, which can be used on the ampoule in the furnace. To rank the different profiles, we use a criterion based on the evolution of the concentration: the time parameter  $\tau$  corresponds to the time when the average concentration in the diluted volume goes over 90% of the average concentration in the ampoule (the average concentration in the whole volume is the same as the concentration obtained after a perfect homogenization of the melt). The lower is  $\tau$ , the faster is the homogenization. In the last part, we will present the viscosity sensibility of our system.

### 5.1 Comparison between constant and variable rotation profiles

An example of VR profile is shown in Figure 4:

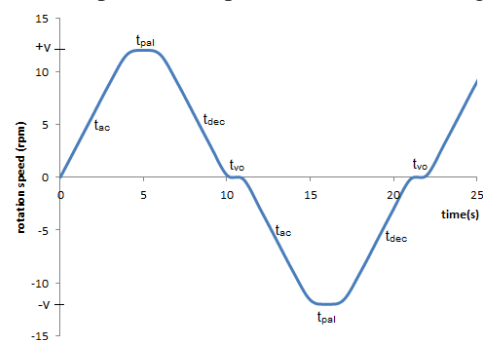


**Figure 4:** Example of VR profile, the angular speed is given in hertz.

In CR profiles, only one parameter can be modified: the speed value. Assuming the geometry of the system and the rotation, we suppose that there is no difference, for the same absolute value, between positive and negative speed in CR profiles (depending on the rotation direction). In VR profiles, we can modify five parameters (shown in the figure 4): max speed  $\pm v$ , time at full speed  $t_{pal}$ , acceleration time  $t_{ac}$ , deceleration time  $t_{dec}$ , and time at 0 rpm  $t_{vo}$ . Several VR profiles were tested: we can first notice that all of them were better than CR with respect to  $\tau$ . The Figures 5 and 6 show the difference in time evolution of the concentration between one CR (12 rpm) and one VR ( $v=12\text{rpm}$ ,  $t_{pal}=1\text{s}$ ,  $t_{ac}=1\text{s}$ ,  $t_{dec}=5\text{s}$ ,  $t_{vo}=0.5\text{s}$ ) profiles.

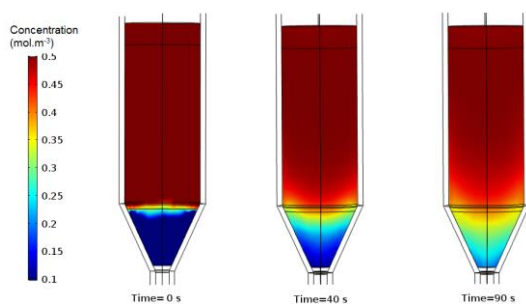


**Figure 5:** Evolution of concentration in the fluid for CR profile (at 0, 40 and 90s), ( $v=12\text{rpm}$ )

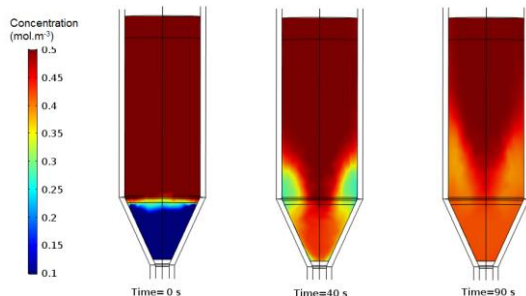


**Figure 6:** Evolution of concentration in the fluid for one VR profile (at 0, 40 and 90s), ( $v=12\text{rpm}$ ,  $t_{pal}=1\text{s}$ ,  $t_{ac}=1\text{s}$ ,  $t_{dec}=5\text{s}$  and  $t_{vo}=0.5\text{s}$ )

Figures 5 and 6 present results from an initial state with low concentration in the bottom but the same kind of results were obtained when low concentration volume is kept in the top in the ampoule. These results seem to indicate that a variable rotation of the ampoule provide a better homogenization in the fluid. So the VR profile has to be optimized.

## 5.2 Optimization of variable rotation profiles

As said in the precedent part, we aimed to reduce the time of homogenization. We have

preferred to keep the speed in the model close to the one used in our experimental part ( $v=12\text{rpm}$ ). We supposed that a too high speed should perturb the crystallization front.

### 5.2.1 Maximum speed influence

The Figure 7 shows the evolution caused by the modification of the max rotation speed parameter in VR profile. The results indicate that the max speed needs to be a intermediate value (around 12rpm) to reduce  $\tau$ . Too small (8rpm) or too high value (20rpm) increases the homogenization time.

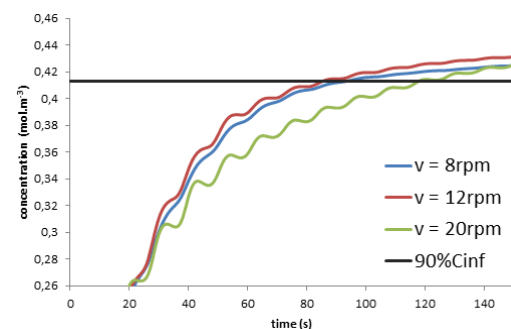


**Figure 7:** Comparison of the evolution of concentration when the max speed is modified ( $t_{pal}=2\text{s}$ ,  $t_{ac}=4\text{s}$ ,  $t_{dec}=4\text{s}$  and  $t_{vo}=1\text{s}$ )

### 5.2.2 Influence of the time duration at max speed

The Figure 8 presents the differences caused by the modification of the duration at max speed. A small value reduces the homogenization time.

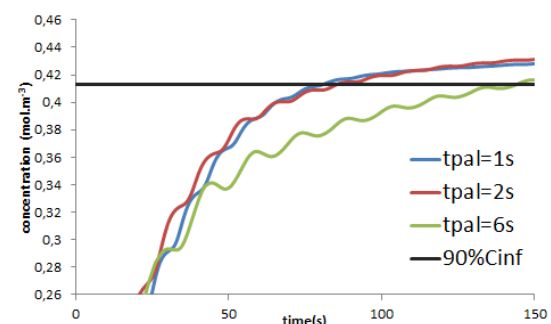


**Figure 8:** Comparison of the evolution of concentration when the dwell time at max speed is modified ( $v=12\text{rpm}$ ,  $t_{ac}=4\text{s}$ ,  $t_{dec}=4\text{s}$  and  $t_{vo}=1\text{s}$ )

### 5.2.3 Time at 0 rpm

The Figure 9 shows the evolution caused by the modification of the dwell time at 0 rpm. A short time value reduces the homogenization time.

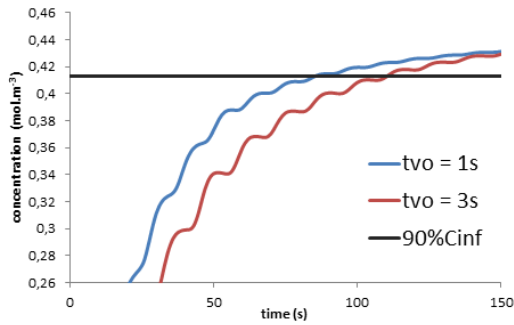


**Figure 9:** Comparison of the evolution of concentration when dwell time at 0 rpm is modified ( $v=12\text{rpm}$ ,  $t_{\text{pal}}=2\text{s}$ ,  $t_{\text{ac}}=4$  and  $t_{\text{dec}}=4\text{s}$ )

#### 5.2.4 Cycle's period effect

Then, the behavior of the system was studied when the total time period was modified. For each profile, we kept the same time ratio between  $t_{\text{ac}}$ ,  $t_{\text{pal}}$  and  $t_{\text{dec}}$ . These three parameters were modified at  $\pm 50\%$  of the value from the initial VR profile ( $t_{\text{ac}}=t_{\text{dec}}=\{2,4,6\}$ ,  $t_{\text{pal}}=\{1,2,3\}$ ). Figure 10 shows the differences related to the modification of the period. Total time period must not be high to obtain a low homogenization time. Small periods gave the same results but one can notice that a 32s period increases drastically  $\tau$  value.

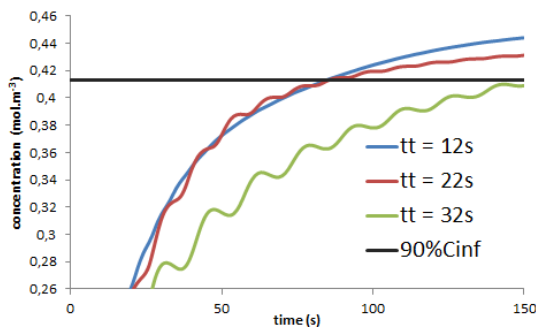


**Figure 10:** Comparison of the evolution of concentration when the cycle's period is modified ( $v=12\text{rpm}$  and  $t_{\text{vo}}=1\text{s}$ )

#### 5.2.5 Dissymmetry between acceleration and deceleration times

The Figure 11 shows the differences observed by a dissymmetry between the acceleration time and the deceleration time. An interesting result was obtained: to perform a faster homogenization, we need to have a short deceleration time and an important acceleration time. A set of two values was used: 1.5s and 4s. In the Figure 11, the ratio  $t_{\text{ac}}/t_{\text{dec}}$  on the graphic represents the ratio between acceleration time and deceleration time:

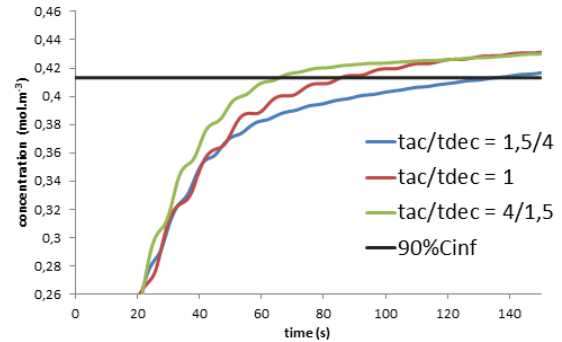


**Figure 11:** Comparison of the evolution of concentration with a dissymmetry between acceleration time and deceleration time ( $v=12\text{rpm}$ ,  $t_{\text{pal}}=2\text{s}$  and  $t_{\text{vo}}=1\text{s}$ )

#### 5.2.6 Summary

In conclusion, a good VR profile must have:

- a medium max speed
- a short dwell time at max speed and at 0 rpm
- a short deceleration time
- a large acceleration time

With these results several profiles were been tested, and  $\tau$  was reduced considerably for the "optimized" VR profile. Figure 12 shows the important difference between the CR at 12rpm and one of the "optimized" profiles ( $v=12\text{rpm}$ ,  $t_{\text{pal}}=1\text{s}$ ,  $t_{\text{ac}}=5\text{s}$ ,  $t_{\text{dec}}=1\text{s}$ ,  $t_{\text{vo}}=0.5\text{s}$ ):

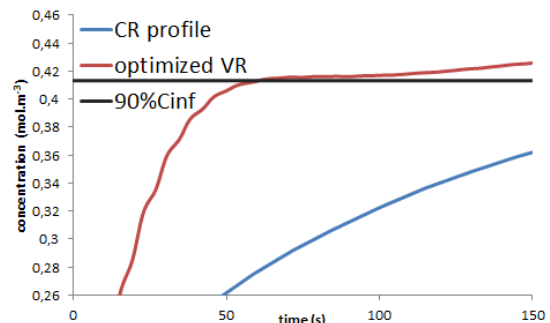


**Figure 12:** Comparison of the evolution of concentration between the CR profile ( $v=12\text{rpm}$ ) and one "optimized" VR profile ( $v=12\text{rpm}$ ,  $t_{\text{pal}}=1\text{s}$ ,  $t_{\text{ac}}=1\text{s}$ ,  $t_{\text{dec}}=5\text{s}$  and  $t_{\text{vo}}=0.5\text{s}$ )

#### 5.3 Influence of the viscosity

As said previously in the Numerical Model Part, the viscosity value for our material is unknown. So we had to approximate the value from related compounds: here Germanium was chosen. The accurate value of the viscosity should probably be different from the chosen one, thus we have studied the influence of the viscosity value variation around the value from pure Germanium.

For a lower viscosity value ( $\mu_0=0.07\text{mPa.s}$ ), no modification on the shapes were observed and the previously optimized VR profile is still good.

In the contrary, for a much higher viscosity, chosen at  $\mu_0=7\text{mPa.s}$ , behavior modifications were clearly seen. Figures 13 and 14 show the evolution of concentration profiles for this high viscosity (same profile rotation than for the figures 5 and 6). First, the VR profile from 5.2.6 (optimized for  $\mu_0=0.73\text{mPa.s}$ ) is not better than the CR profile ( $v=12\text{rpm}$ ). Second, the system have better homogenization with a large time at full speed and with a short acceleration time. This is in an opposite behavior than the one observed with a lower viscosity ( $\mu<1\text{mPa.s}$ )

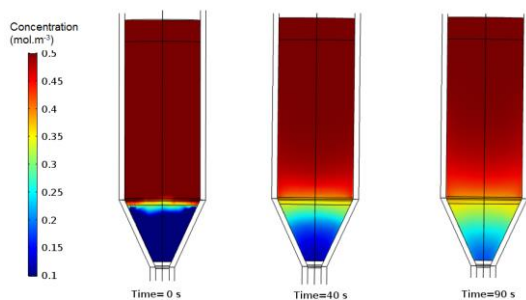


**Figure 13:** Evolution of concentration for CR in the fluid, with high viscosity (at 0, 40 and 90s), speed of 12rpm

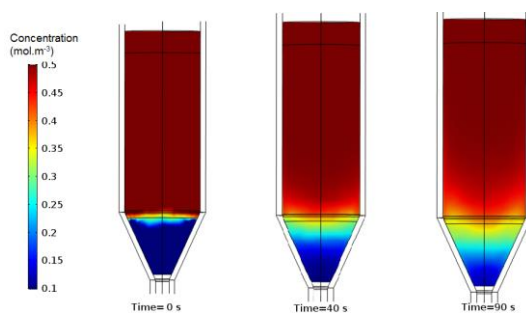


**Figure 14:** Evolution of concentration for one VR profile in the fluid, with higher viscosity (at 0, 40 and 90s), ( $v=12\text{rpm}$ ,  $t_{\text{pal}}=1\text{s}$ ,  $t_{\text{ac}}=1\text{s}$ ,  $t_{\text{dec}}=5\text{s}$  and  $t_{\text{vo}}=0.5\text{s}$ )

The Figures 15 and 16 show the difference between a CR ( $v=12\text{rpm}$ ), one of the first VR profile used (Fig 6), the “optimized” VR profile from the 5.2) at a viscosity of  $0.73\text{mPa.s}$  for the Figure 15 and at a viscosity of  $7\text{mPa.s}$  for the Figure 16.

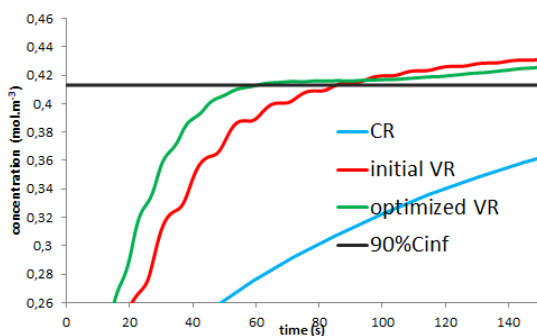


**Figure 15:** Comparison of the evolution of concentration in the initial viscosity ( $\mu_0=0.73\text{mPa.s}$ ) between CR, an initial VR and “optimized” VR

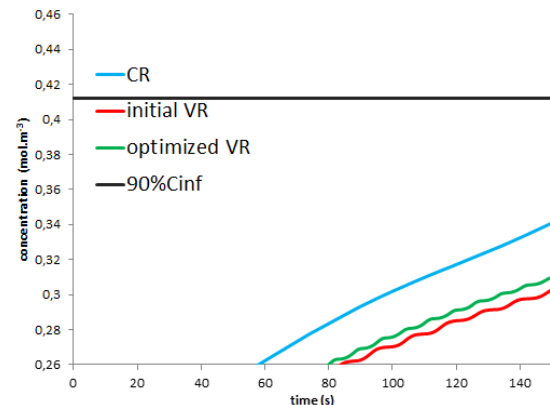


**Figure 16:** comparison of the evolution of concentration in high viscosity ( $\mu_0=7\text{mPa.s}$ ) between CR, an initial VR and “optimized” VR

Optimization of VR profiles with high viscosity ( $\mu_0=7\text{mPa.s}$ ) should be further performed, as the VR profiles tested are not appropriate.

## 6. Conclusion

Comsol Multiphysics<sup>TM</sup> was used to study the homogenization behavior in a rotated ampoule for a Bridgman-Stockbarger furnace. Even though some values were approximated (because no data are available for our composition at high temperature), the simulation shows that a variable rotation profile of the ampoule results in a shorter homogenization time than in the constant rotation profile, for the chosen viscosity ( $\mu_0=0.73\text{mPa.s}$  at  $1000^\circ\text{C}$ ). After studying the modification of behavior by varying the different parameters in the variable rotation, the variable rotation profile was optimized. However the simulations show a modification of behavior when the viscosity of the fluid is high ( $\mu_0=7\text{mPa.s}$ ): the variable rotation profile optimized for a low viscosity is not better than the constant rotation for a high viscosity melt.

In order to further optimize the rotation parameters for our experiments, the value of the viscosity of our compounds versus the temperature must be experimentally determined. As the viscosity of our compound might be close to  $7\text{mPa.s}$ , we need to optimize the rotation profile for such a high viscosity. In a second time, to improve the homogenization again, we could use our model to optimize the ampoule geometry.

## Acknowledgement

We would like to acknowledge the DGA (Direction General de l'Armement) for their funding support of our work.

## Reference

- 1 D.M Bubb, J.S. Hortwiz, M.R. Papantonakis, R.F. Haglund; Resonant infrared pulsed laser deposition of polymers using a picosecond tunable free-electron laser. *Opt. Soc. America*, p94-95 (2002)
- 2 A. Godart; Infrared (2-12 $\mu$ m) solide-state laser sources: a review, *Comptes rendus Physique*, **8(10)**, p1100-1128 (December 2007)
- 3 V. Petrov; Parametric down-conversion devices: The coverage of the mid-infrared spectral range by solid-state laser sources, *Optical Materials*, **34(3)**, p536-554, (2012)
- 4 G. Overton; Photonic frontiers: Laser countermeasures: Scaling down mid-IR laser countermeasures for smaller aircraft, *Laser Focus World*, **50(4)**, p31-38, 2014
- 5 P. Larkin; Infrared and Raman spectroscopy: principles and spectral interpretation, Elsevier, Amsterdam; Boston (2011)
- 6 Y.M. Andreev, P.P. Geiko, A.V. Shaiduko, J. Gao, T. Ma, Y. Jiang, S.G. Grechin; New possibilities in design of femtosecond light sources for lidar applications, *Proc. Of SPIE*, **5027**, p128-135 (2003)
- 7 D.J. Knuteson, N.B. Singh, G. Kanner, A. Berghmans, B. Wagner, D. Kahler, S.McLaughlin, D. Suhre, M. Gottlieb; Quaternary AgGaGe<sub>n</sub>Se<sub>2(n+1)</sub> crystals for NLO applications, *Journal of Crystal Growth*, **312**, p1114-1117 (2010)
- 8 J. Petit, M. Bejet, J-C. Daux; Highly transparent AgGaS<sub>2</sub> single crystals, a compound for mid IR laser sources, using a combined static/dynamic vacuum annealing method, *Materials Chemistry and Physics*, **119**, p1-3 (2010)
- 9 J. Petit, A. Godard, M. Raybaut, J-M. Melkonian, M. Lefebvre; Mid-IR non-linear material: chemical synthesis, crystal growth and Difference Frequency Generation in ZnGeP<sub>2</sub> and AgGaS<sub>2</sub>, *Proc of SPIE*, **vol 7838**, p78811 (2010)
- 10 J. Rame, B. Viana, Q. Clément, J-M. Melkonian, J. Petit; Control of Melt Decomposition for the Growth of High Quality AgGaGeS<sub>4</sub> Single Crystals for Mid-IR Laser Applications, *Crystal Growth and Design*, **14**, p5554-5560 (2014)
- 11 G. Anandha Babu, R. Subramaniyan, N. Karunakaran, R. Perumal Ramasamy, P. Ramasamy, S. Ganesamoorthy, P.K. Gupta; Growth improvement of AgGaSe<sub>2</sub> single crystal using the vertical Bridgman technique with steady ampoule rotation and its characterization, *Journal of Crystal Growth*, **338(1)**, p42-46 (2012)
- 12 P. Rudolph, M. Neubert, M. Mühlberg; Defects in CdTe Bridgman monocrystals caused by nonstoichiometric growth conditions, *Journal of Crystal Growth*, **128**, p582-587, (1993)
- 13 D.S. Snaditov; Deformation-activation model of viscous flow of glass-forming liquids, *Journal of Non-Crystalline Solids*, **400**, p12-20 (2014)
- 14 L. Battezzati, L. Greer; The viscosity of liquid metals and alloys, *Acta metal.*, **Vol. 37, No7**, p 1791-1802 (1989)
- 15 D. Lide; *CRC Handbook of chemistry and physics*, 2804p, CRC Press Inc. (2009)